Interaction Between Typhoon and Western Pacific Subtropical Anticyclone: Data Analyses and Numerical Experiments*

Ren Suling[1,2](任素玲), LIU Yimin[3†](刘屹岷), and WU Guoxiong[3](吴国雄)

1 *National Satellite Meteorological Center, China Meteorological Administration, Beijing* 100081

2 *Graduate University of Chinese Academy of Sciences, Beijing* 100081

3 *State Key Lab of Atmospheric Sciences and Geophysical Fluid Dynamics (LASG), Institute of Atmospheric Physics, Chinese Academy of Sciences, Beijing* 100029

(Received October 30, 2008)

ABSTRACT

Three kinds of typhoons with distinct tracks are sorted based on a set of typhoon data from 1958 to 1998. The results of composite analyses confirm that different typhoon tracks correspond to different patterns of the subtropical anticyclone over the western Pacific (SAWP). When the tracks are westward, the SAWP is strong, with a zonal form, and stretches westward; when the tracks are recurving, the main body of the SAWP shifts eastward and breaks near 160°E; and when the tracks are northward, the SAWP is located far east of its normal position. Based on the above result, two different initial fields are configured, one has a zonal and strong SAWP, and the other has a meridional and weak SAWP. By using the GOALS R42L9 climate model, a temperature disturbance is added into these two different initial fields to force the formation of a typhoon. Westward and northward tracked typhoons are well simulated, thus verifying that different patterns of the SAWP have different effects on typhoon tracks. Results also show that typhoons can induce barotropic Rossby waves propagating to the mid and high latitudes. Under different background zonal flows, the wave trains triggered by the typhoons of westward and northward tracks are also different, and their effects on the mid and high latitude circulations and the SAWP are different. Compared to a northward tracked typhoon, a westward tracked typhoon is able to induce positive geopotential height anomaly to its north and northwest, resulting in the SAWP strengthening and developing westward.

Key words: typhoon, subtropical anticyclone over the western Pacific (SAWP), interaction, numerical experiment

1. Introduction

Tropical cyclone is one of the important systems that influence the summer weather in China. There have been a series of thorough studies on its distribution, structure, and interaction with different scale systems. The results show that the large scale flow is the most important factor that affects the movement of tropical cyclone, such as the variation of the SAWP, ITCZ (intertropical convergence zone) break, equatorial buffer zone's activity, planetary wave's transformation from meridional to zonal pattern, and the transformation from trade wind to monsoon. Wu and Wang (2000) thougt that tropical cyclone can be taken as a positive potential vorticity (PV) anomaly in the steering flow associated with the SAWP, and its moving direction is related to the tendency of the positive potential vorticity. Studies on lager-scale steering flow also show that the track of typhoon has a good relationship with the wind averaging from upper to low levels, especially the average wind fields at 700, 600, and 500 hPa. Harr and Elsberry (1991) studied the relationship between the tracks of the tropical cyclone and the anomaly of large-scale wind flows, and found that there is a good relationship between them at 700 hPa. Synoptic scale systems can also affect the abnormal movement of the tropical cyclone (Fan, 1996; Dong and Neumann, 1983; Luo and Ma, 2001; Chen and Luo, 1995). The SAWP is one of the most important factors which influence the tracks of the tropical cyclone, through its corresponding steering flow (Zhu et al., 1992; et al. 1991).

*Supported jointly by the National Key Basic Research Developing Program of China (2004CB418300), and the National Natural Science Foundation of China under Grant Nos. 40575028 and 40523001.

†Corresponding author: lym@lasg.iap.ac.cn.

The intra-annual variations of the SAWP can be categorized at three different time scales, i.e., the seasonal variation, the longer period variation of about 15 day, and the short period variation of about one week. Pervious studies usually focused on the impacts of the surrounding large-scale systems on the SAWP, such as South Asian anticyclone, East Asian summer monsoon, mid-high latitude westerly flow, and the ITCZ. Is there any effect of typhoon on the variations of the SAWP through heavy rainfall associated strong latent heating? Former studies (Yu and Pan, 1989; Qian and Yu, 1991; Zhang et al., 1995; Wu et al., 1999; Liu et al., 1999, 2001; Rodwell and Hoskins, 2001) showed that the latent heating of East Asian monsoon rainfall has an important effect on the variations of the SAWP. Nikaidon (1989) also pointed out that the rainfall over the tropical western Pacific can intensify the SAWP. Hoskins and Karoly (1981) addressed that thermal forcing from latent heat release can generate Rossby waves propagating polewards. Few scientists focused their eyes on the effect of typhoon on the variations of the SAWP through latent heating during short time periods. We can suppose that the tropical cyclones happening frequently in summer should also have important effects on the variations of the SAWP because of the latent heat release. In this paper, the authors attempt to understand the interaction between the tropical cyclone and the SAWP by using composite analyses and numerical experiments.

2. Data and method

2.1 *Typhoon and atmospheric data*

The typhoon data are provided by China Meteorological Administration, including genesis time, central position, lowest central pressure, and maximum velocity of the cyclonic winds, four times per day at 0200, 0800, 1400, and 2000 UTC, respectively. Other atmospheric data are from NCEP/NCAR including daily pressure and surface data, with the resolution of $2.5°\times2.5°$ except for precipitation which is $1.875°\times1.875°$, and these data are taken 4 times per day at 0000, 0600, 1200, and 1800 UTC. In the following analyses, the position at 0200 UTC is regarded as the typhoon position of the day, and the corresponding geopotential height and wind fields are at 0000 UTC.

2.2 *The composite of the atmospheric flow field*

Previous studies showed that the tracks of tropical cyclones are not only influenced by the steering flow but also by some other occasional factors, thus the composite method is used to eliminate the influence of small-scale factors on the tracks of tropical cyclones. The strength of the steering flow also has a close relationship with the position and strength of the SAWP, thus the composite method can highlight the prominent and common factors so as to explore the relationship between the tropical cyclone and the SAWP in a better way. In order to describe the circulation fields and the precipitation when typhoons happen, all typhoons are adjusted to the average position at the corresponding time (Fig.1d). The geopotential height, wind, and precipitation in three typical categories of typhoon cases are also adjusted accordingly. The latitude and longitude refer to those of the average fields after the adjustment.

2.3 *The choice of three typical categories of typhoon cases*

Typhoons happening in the northwestern Pacific are divided into three typical categories according to their different tracks in this study, i.e., the westward and northwestward tracks, the recurving tracks, and the northward tracks. Typhoon cases in this paper are chosen in July and August of 1958–1998. There are 23 cases for those with the westward and northwestward tracks, and these 23 typhoons have numbers in Fig.1a as 6219, 6310, 6313, 6318, 6412, 6517, 6724, 6815, 6817, 6907, 7118, 7119, 7121, 7218, 7617, 7706, 7911, 8012, 8209, 8210, 8213, 8303, and 9714 (in Typhoon Annals), and most of them are landfall typhoons. There are also 23 cases with recurving tracks, and their numbers in Fig.1b are 6522, 6213, 5906, 6521, 6808, 6411, 6311, 7217, 6210, 6714, 8009, 8708, 7810, 5822, 6912, 6621, 6220, 7918, 9310, 8714, 9010, 9503, and 9211, and most of them recurved over the ocean. The lifetime of the northward tracked typhoons is usually shorter than that of the other two kinds of typhoons. To compare the three kinds of

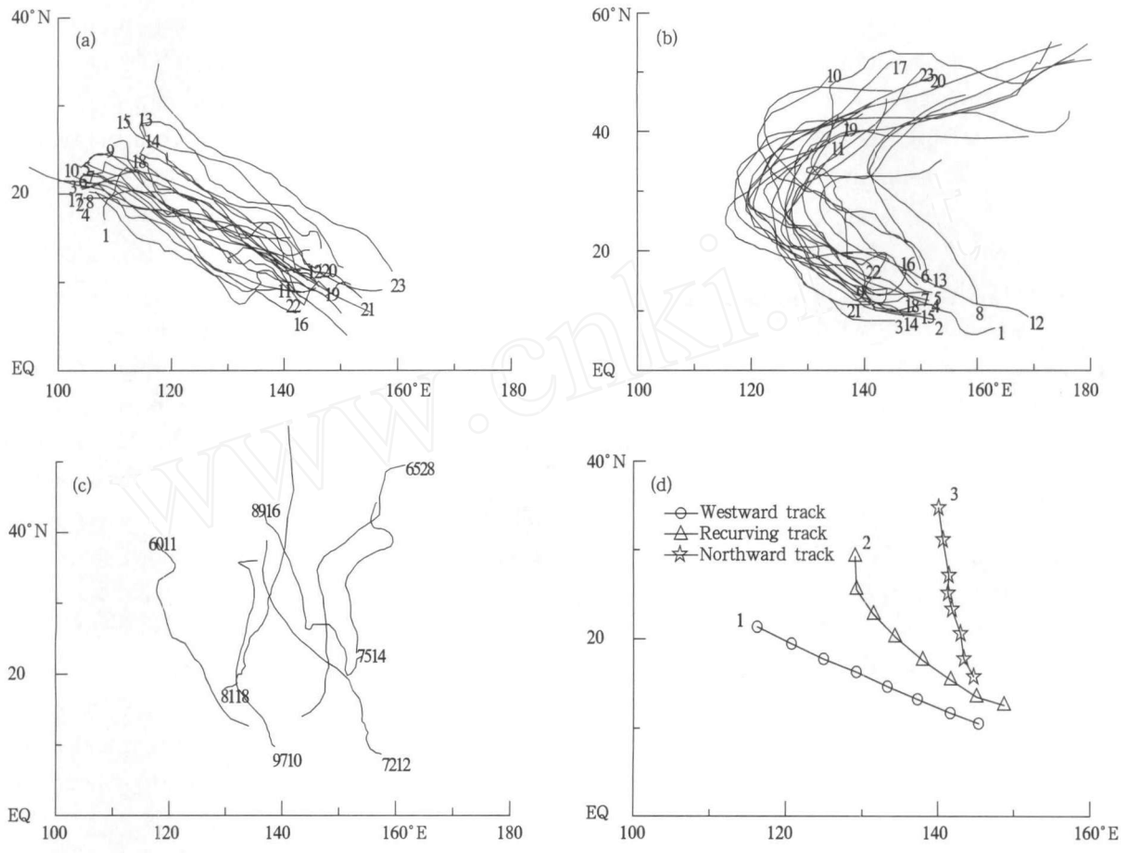

Fig.1. Average tracks of three typical categories of Northwest Pacific typhoon cases (numerals of 1–23 are the typhoon number in (a, b) and the directly labeled numbers are given in (c)). (a) Westward and northwestward tracks; (b) recurving tracks; (c) northward tracks; and (d) average tracks of the westward and northwestward, the recurving, and the northward at 0200 UTC for the first eight days, respectively.

typhoons, we only choose those whose lifetime is longer than or equal to 8 days, and whose tracks spread not too widely compared with the other two types. The occurrences of northward tracked typhoons are fewer than the other two kinds of typhoons and their tracks are distributed in a wide range in longitude. For these reasons there are only seven cases with the northward tracks (Fig.1c). The average daily positions for the three kinds of tracks are shown in Fig.1d.

From Fig.1d we can find that the westward and northwestward tracked typhoons move faster than the other two kinds. The northwestward ones move slower in the first six days and normally in the last two days. The westward and northwestward (called westward for short) tracked typhoons originate at almost the same longitude as that of the northward ones near 145°E, but at 10.5°N, which is to the south of the originating place of the northward tracked typhoons. The recurving tracked typhoons originate at about 150°E, and recurve at about 26°N, 130°E. The originating place of northward tracked typhoon is the most north among three kinds of typhoons. The first day position of the typhoons is at 10°, 12°, and 15°N for the westward, recurving, and northward tracked typhoons, respectively.

3. Patterns of the SAWP corresponding to three different typhoon tracks

Figures 2, 3, and 4 are geopotential height and wind fields at 500 hPa every other day for the westward, recurving, and northward tracked typhoons. The geopotential height greater than 5880 gpm is shaded, representing the main part of the SAWP. The

results show that the typhoons with different tracks correspond to different patterns of the SAWP.

When the tracks are westward (Fig.2), initially the corresponding SAWP is oriented zonally and it develops strongly. The zonal wind north of the SAWP is smooth with no significant waves. The strength of the western part of the SAWP is weak and its area is becoming small when the typhoon located south of the SAWP starts to move westward in the easterly during the first couple days. On the fourth day, when the typhoon moves to the west of the SAWP, the strength of the western part of the SAWP reaches the minimum, but the SAWP does not extend zonally. From the fifth to the eighth day, the westward extending point of the SAWP moves westward from 134°E on the fourth day to 124°E on the eighth day, the SAWP stretches westward obviously, its western part develops meridionally, and the range of the SAWP extends to north when the typhoon moves westward in this period.

When the tracks are recurving (Fig.3), the main body of the SAWP tends to be eastward and its meridional development is weaker than that of the westward tracks during the lifetime period. At the typhoon center in about 150°E there is a trough in mid-high latitude zonal flows, and the zonal SAWP becomes narrower at 150°E. From the second day, the SAWP becomes weak. On the fourth day when the typhoon is located at the west of the SAWP, the strength of the SAWP develops strongly in longitude. On the fifth day, the trough in the westerlies north of the SAWP develops gradually, and the main body of the SAWP breaks near 160°E. On the seventh day, the typhoon begins to recurve, and at the same time, the trough over the East Asian Continent also moves to about 120°E. Thus, the same conclusion as the former paper by Wang (1981) comes by, that is, most of the typhoons would recurve over the ocean when there is a trough at about 120°E. Further studies show that the sudden development, weakening, replacement, and retreat of troughs here have impacts on typhoon tracks. As a whole, if the main body of the SAWP is farther east than normal, it is in favor of the recurving tracked typhoons over the ocean. The trough and ridge in westerlies would develop when a typhoon is to the west of the SAWP.

When the tracks are northward (Fig.4), the

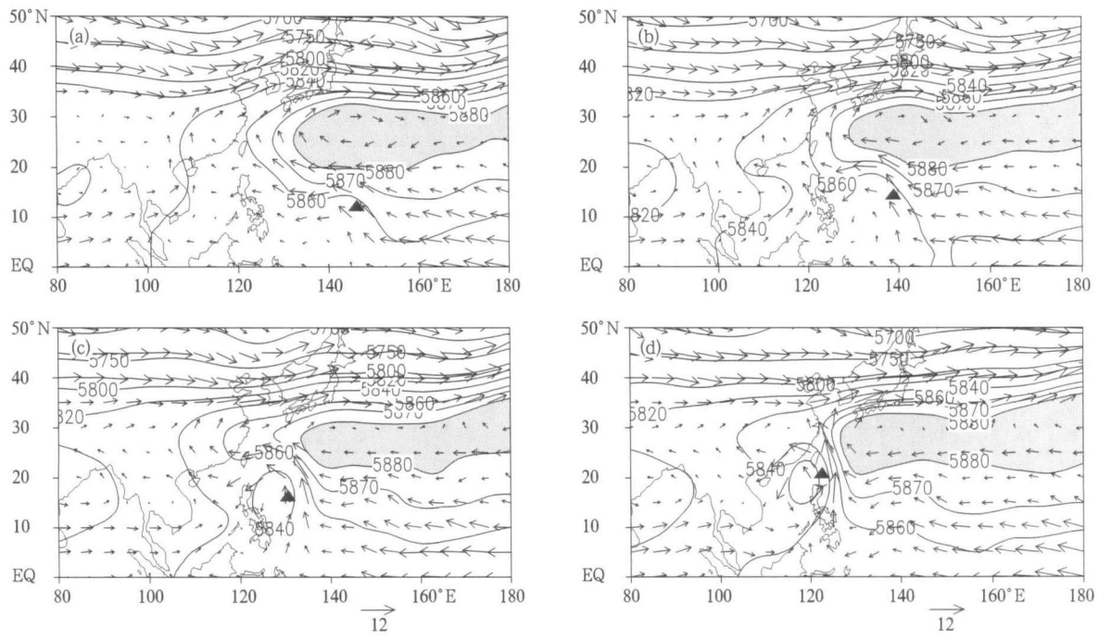

Fig.2. The 0000 UTC 500-hPa geopotential height field (solid line, the interval is 50/20 gpm when the geopotential height is greater/less than 5800 gpm, respectively, and the geopotential height greater than 5880 gpm is shaded) and wind field (vector, m s^{-1}) for the westward tracks. ▲ represents the typhoon center at 0200 UTC. (a) The first, (b) third, (c) fifth, and (d) seventh day.

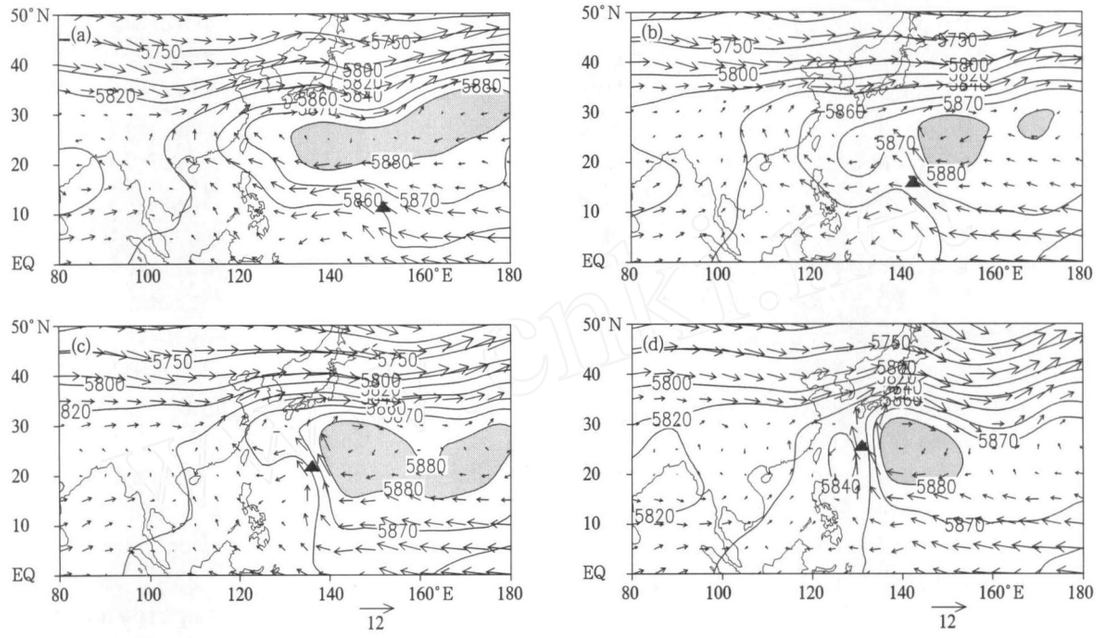

Fig.3. As in Fig.2, but for the recurving tracks.

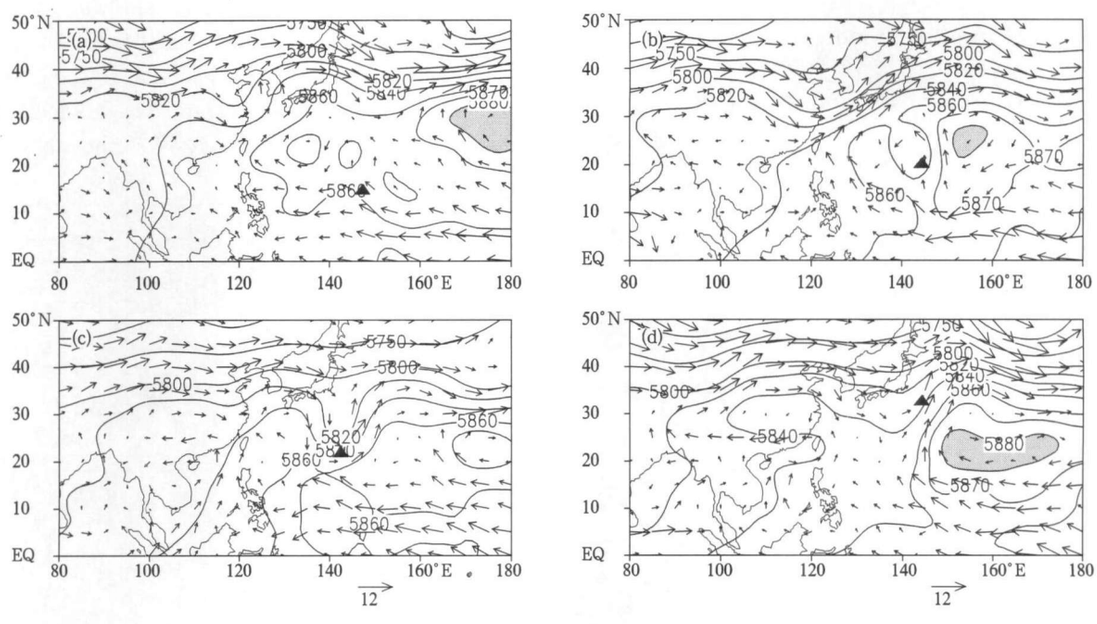

Fig.4. As in Fig.2, but for the northward tracks.

SAWP is located in the far east of the Pacific and its intensity is the weakest. There are significant waves in the westerlies. A shallow trough is found at about 120°E in East Asia on the first day, and then begins to develop on the second and the third day. The trough moves suddenly to the east and incorporates with the typhoon low-pressure system on the fourth day. From the fifth day, the SAWP to the east of the typhoon begins to intensify along with the northward migration of the typhoon and the western part of the SAWP stretches to the north, the anticyclonic circulation west of the typhoon is also intensified and forms a small anticyclonic pressure center of 5860 gpm till the eighth day. As a whole, the circulation of the SAWP

north of the typhoon would break into two separate anticyclonic centers when the northward tracked typhoon moves northward to the south of the SAWP, and the typhoon gets through the area of low pressure between the two anticyclonic centers. When the typhoon moves to the north of the SAWP, the anticyclone circulation east of the typhoon will intensify suddenly which can induce the sudden westward outspreading of the SAWP after the typhoon passes by.

The composite analyses show that there is a close relationship between these three typical categories of typhoon tracks and the patterns of the SAWP, which is in accordance with the former case studies (Liu and Liang, 1987). In order to validate the conclusion and explore the effect of three different typhoon tracks on the SAWP, numerical experiments by using a climate model are conducted to simulate the effect of the different patterns of the SAWP on typhoon tracks and discuss the mechanism of the possible effects for the typhoon on the SAWP.

4. Numerical experiments

4.1 *Description of the numerical model*

The climate model LASG/IAP GOALS R42L9, developed from R15L9, is used in this paper. The atmospheric model has a horizontal resolution of 2.8125°(longitude)×1.66°(latitude), and nine levels in the vertical in σ-coordinates. The land surface model is the SSiB model (Liu and Wu, 1997; Xue et al., 1991). The radiation process is the K-scheme by Shi (1981), updated once per 6 h. The ocean model was switched off in the numerical experiments, and the solar zenith angle was taken constant as that on 15 July. The initial fields are that of 1 January 1978, and the model was integrated for 4 yr in the control run. The results on days 271 and 63 in the fourth year of the Atmosphere Model Intercomparison Project (AMIP) Experiment (integration started from 1 January 1978) are chosen as the initial fields of the sensitivity runs for the westward tracked typhoon and the northward tracked typhoon, respectively. This is because the 500-hPa geopotential height field is in a zonal form over the western Pacific, i.e., there is a zonal SAWP on day 271 (Fig.5), which is similar to the observed initial field of the westward tracked typhoon (Fig.2a); and the 500-hPa geopotential height show that the SAWP breaks near Japan on day 65 (Fig.5c), similar to the observed initial field of the northward tracked typhoon (Fig.4a). The integration period is 10 days for the above two

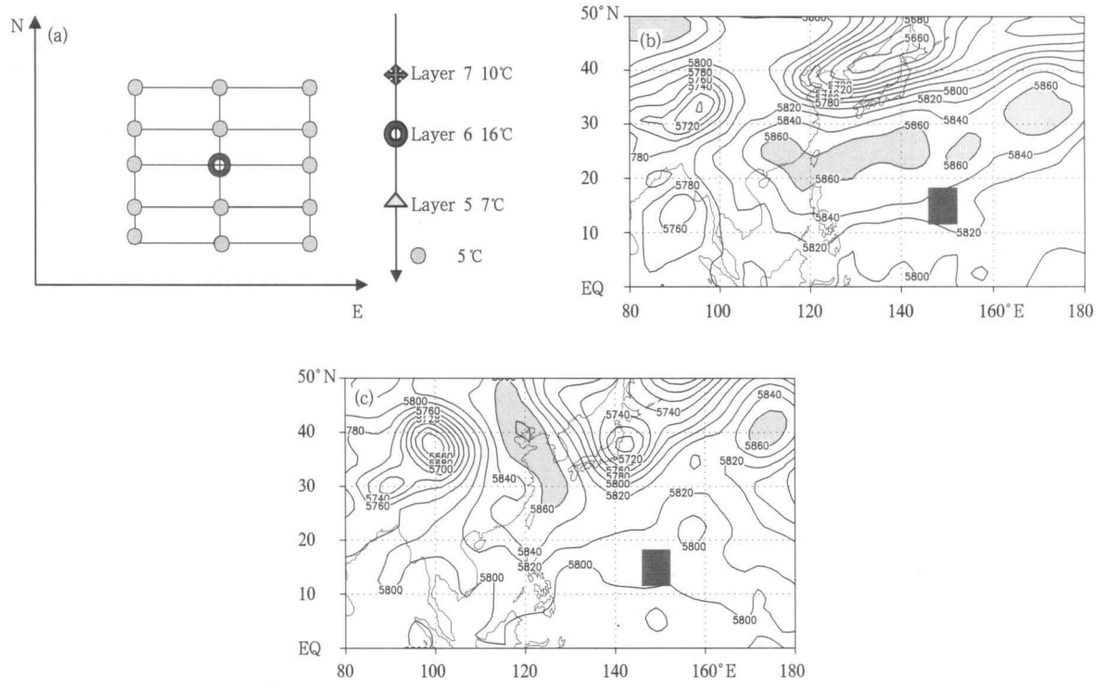

Fig.5. (a) Configuration of the temperature disturbance added to the sensitivity experiments; (b) and (c) are the initial fields of 500-hPa geopotential height for Experiments 1 and 2, respectively, with the geopotential height greater than 5880 gpm shaded and the initial position of temperature disturbances denoted by a black-rectangle.

experiments (Experiments 1 and 2).

4.2 *Experiment design*

A temperature disturbance as shown in Fig.5a is added into initial fields of the two experiments based on the observed cumulus latent heating profile of the typhoon. One rectangle (6.68° in longitude, 5.625° in latitude) temperature disturbance is added into the sixth model vertical layer (i.e., 336 hPa). The maximum disturbance at the center is 16°C, and the disturbance at the surrounding 14 grids is 5°C. A temperature disturbance of 10°C is added to only one grid at the center of the seventh model vertical layer, and that of 5°C to the center of the fifth model layer. The heating center grids are (54, 45), that is, (14.85°N, 149.0625°E). The added temperature disturbance is equivalent to a positive potential vorticity at the upper troposphere according to the invertibility principle of potential vorticity (Hoskins et al., 1985). The result shows that this kind of initial force can ignite a typhoon rapidly in the lower atmosphere.

5. Simulated interaction between typhoon and the SAWP

The temperature disturbance in Fig.5a is added to the rectangle areas of the initial fields in Figs.5b and c, respectively, and then the model is integrated for 10 days. The 850-hPa geopotential height and wind from the second day to the fourth day are shown in Fig.6. The maximum positive vortex position (indicating the typhoon position) at 850-hPa in the first five days are also marked in Fig.6. It shows that the initial temperature disturbance is able to ignite two strong typhoons in the two experiments: the geopotential height is lower than 1280/1160 gpm at the center of the northward/westward tracked typhoons at 850 hPa. We can get some conclusions about the interaction between typhoon and the SAWP in bellow:

(1) In Experiment 1 for westward tracked typhoon, the typhoon landed on day 5. In Experiment 2, the track was westward in the first two days, and then began to move northward in the following days, which was corresponding to the northward tracked typhoon. This result is consistent with that from the composite analysis. It verifies the traditional view that westward and north-westward typhoon tracks are favored when the SAWP is in a zonal form, but northward typhoon tracks are favored when the SAWP breaks in its middle part.

(2) In Experiment 1 for the westward tracked typhoon, the main part of the SAWP and its ridge developed westward with the typhoon moving westward. In Experiment 2 for the northward tracked typhoon, the main body of the SAWP was located more east and seldom moved. This shows that different types of typhoon tracks can be attributed to different patterns of the SAWP.

6. A possible mechanism of typhoon affecting the variation of SAWP

In order to analyze the effect of typhoon on the SAWP, the differences of 500-hPa geopotential height between the sensitivity experiment and the control run for Experiments 1 and 2 are shown in Fig.7. The change of 500-hPa geopotential height denotes the influences by the typhoon. Figure 7 shows that 500-hPa geopotential height decreased in the west of the heating source on day 1 for westward and northward tracked typhoons, and the change in intensity and area of 500-hPa geopotential height was almost the same for the two kinds of typhoon tracks. From day 2, the geopotential height near Japan and east of Japan began to increase in the two experiments. By day 3, there was an obvious difference between Experiments 1 and 2. In Experiment 1, the geopotential height increased near Japan, and the positive area expanded northwestward. Meanwhile, there appeared another area with comparable height increase in the northwest (area III in Fig.8). In Experiment 2, the geopotential height increased greatly up to 80 gpm in area I, but the positive area did not expand westward. In the following three days, the geopotential height increased gradually and the positive area expanded southeastward (Fig.7a$_3$). There was westerly wind in area III all the time in Experiment 1 (Fig.6a), but in Experiment 2, there was easterly wind all the time (Fig.6b), and the geopotential heights changed little in area III.

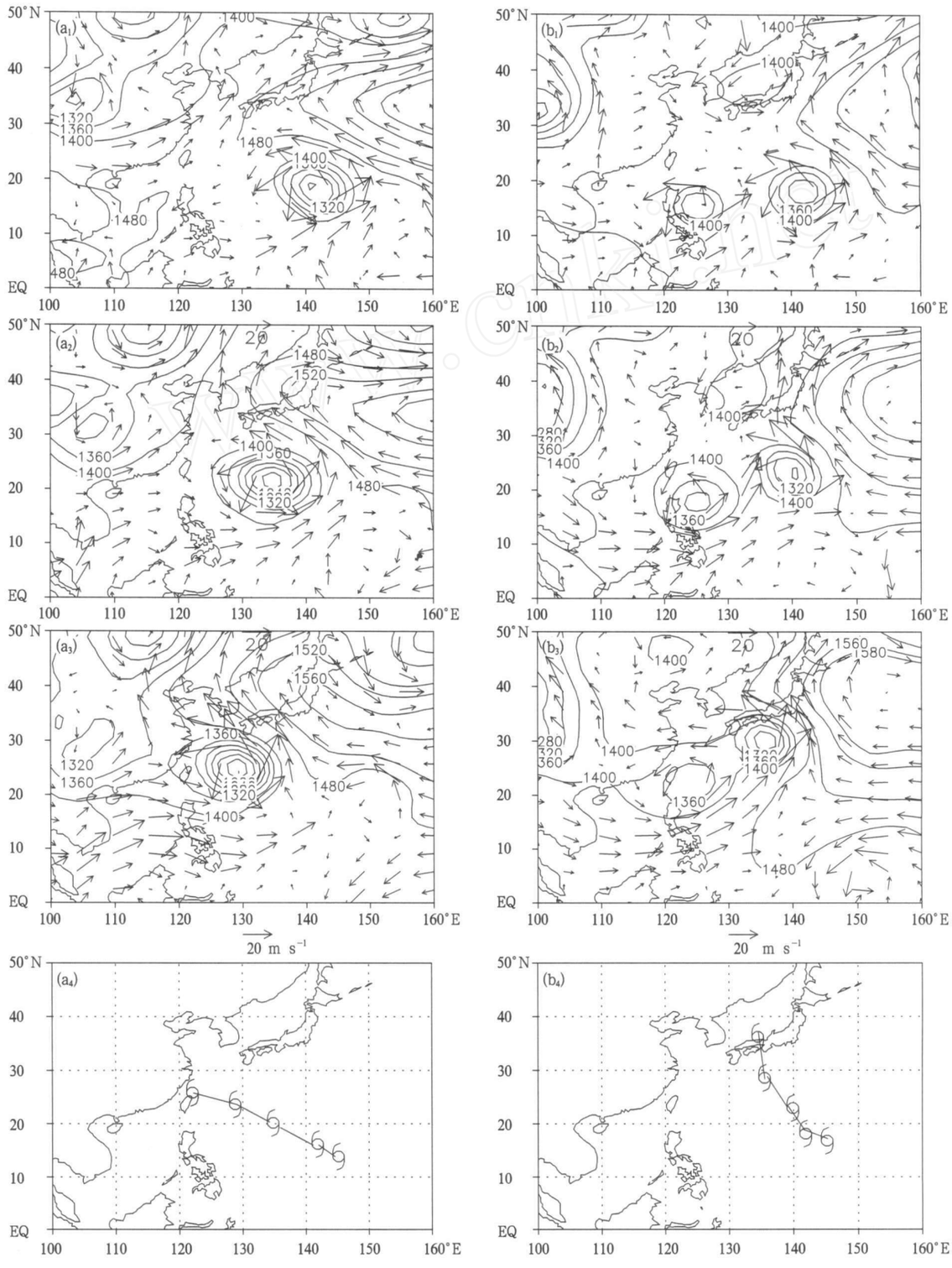

Fig.6. The 850-hPa geopotential height fields (solid line, the interval is 20/40 gpm when the geopotential height is greater/less than 1440 gpm, respectively) and wind fields (vector, m s^{-1}) on the second (a_1,b_1), third (a_2,b_2), and forth (a_3,b_3) day from simulation Experiments 1 (left panels) and 2 (right panels). The tracks of maximum vorticity centers from the first to fifth day in the two experiments are shown in the two bottom panels (a_4,b_4), respectively.

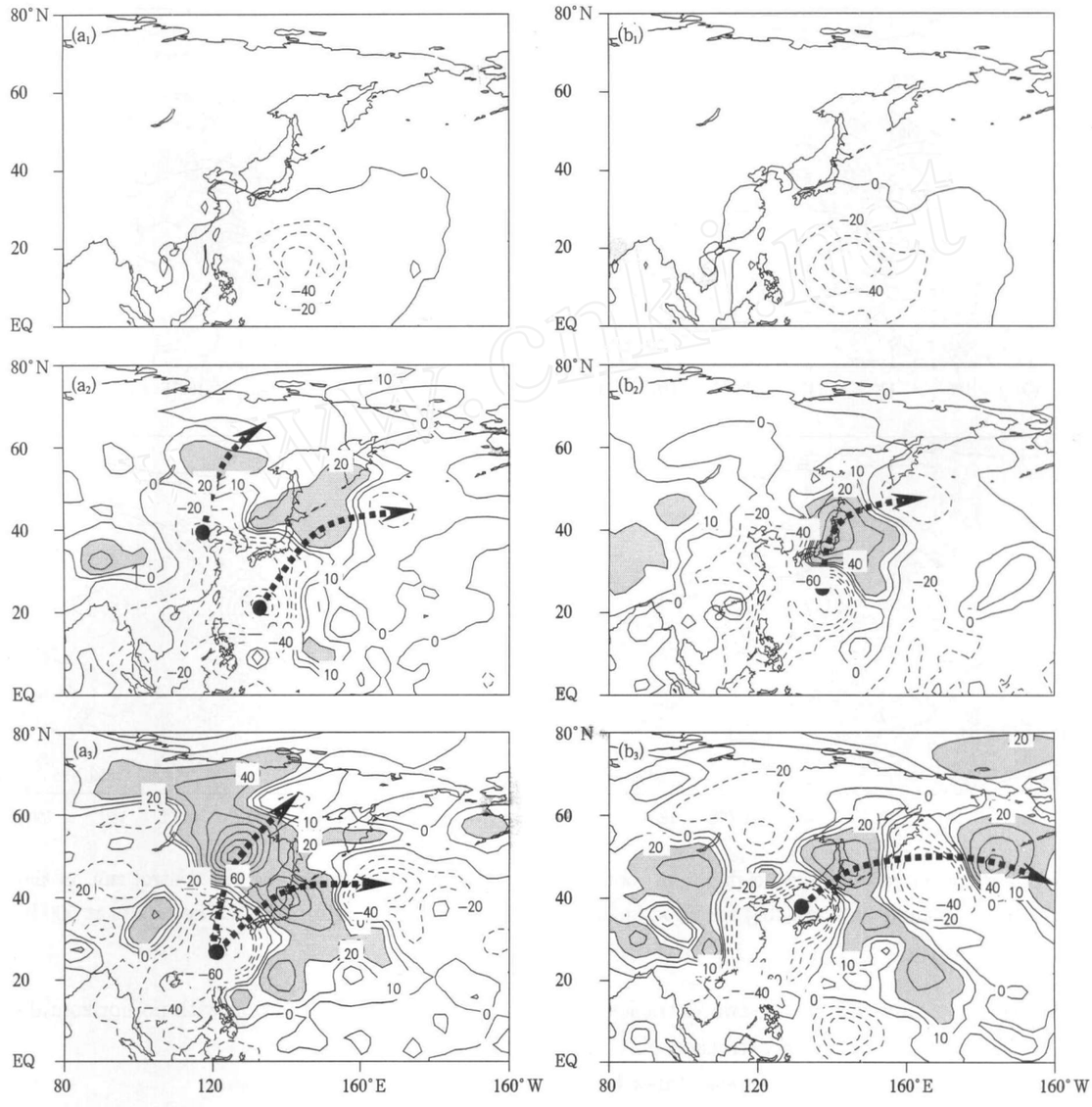

Fig.7. Differences of 500-hPa geopotential height (gpm) between the sensitivity experiment and the control run on the first (a_1,b_1), third (a_2,b_2), and fifth (a_3,b_3) day for Experiments 1 (left panels) and 2 (right panels). Differences greater than 20 gpm are shaded, and dashed arrows indicate energy transport tracks.

To sum up, for the westward tracked typhoon, there were two geopotential height increase areas concurring with a westward moving height decrease area of the typhoon. One of the two positive areas was in the northwest-north and the other was in the northeast, corresponding to two obvious wave trains. There were two negative centers in the front (east) of the energy transport path. But for the northward tracked typhoon, there was only one positive and one negative geopotential height difference centers at 500 hPa in the northeast along the energy transport path corresponding to one obvious wave train. It is shown that the SAWP stretched to the west and its intensity increased because there was one positive center to the northwest of the westward tracked typhoon (Fig.6a). But for the northward tracked typhoon, the SAWP is located further east with no westward stretching (Fig.6b).

Figure 8 shows the vertical distribution of geopotential height differences in Experiments 1 and 2 at 200 and 850 hPa (for 500 hPa, seen in Figs.7a_2, b_2). We can find that the geopotential height difference near the typhoon is positive at 200 hPa but negative at 500

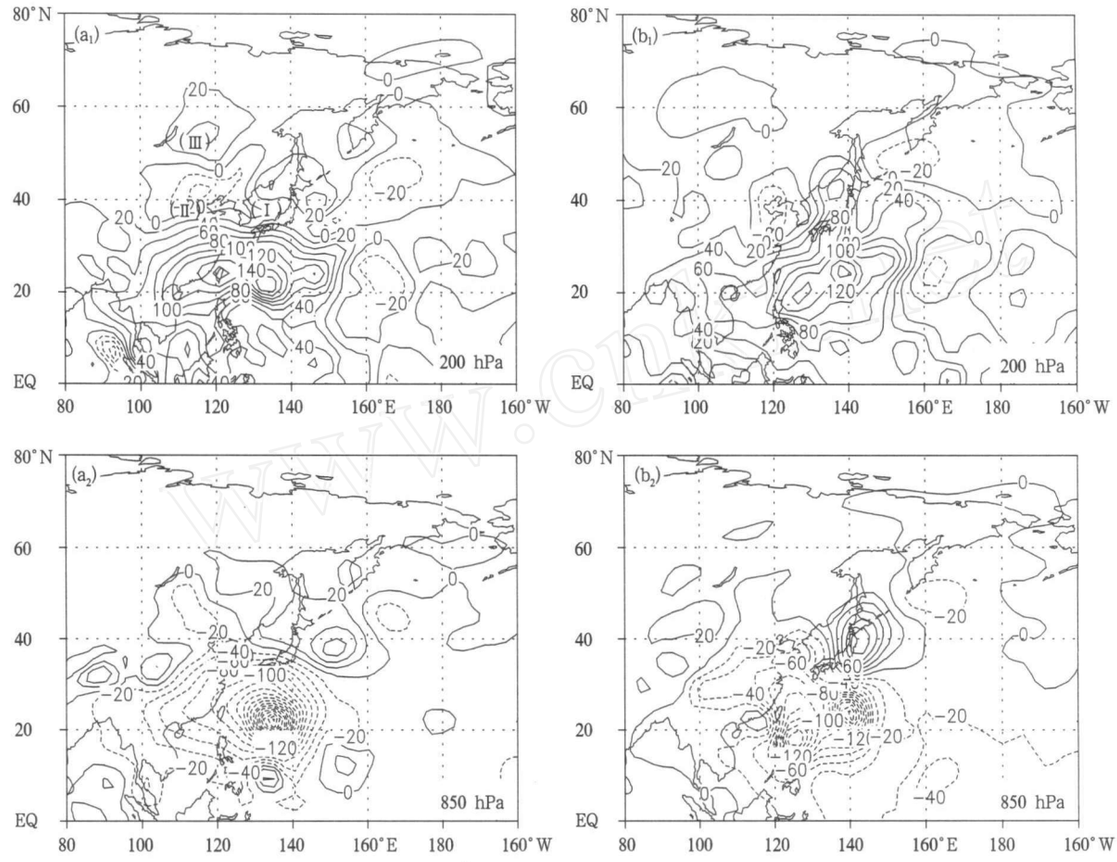

Fig.8. Differences of geopotential height (gpm) between the sensitivity experiment and the control run on the third day at 200 (a_1,b_1), and 850 hPa(a_2,b_2) for Experiments 1 (left panels) and 2 (right panels). The results at 500 hPa are shown in Fig.7 (a_2, b_2).

and 850 hPa not only for the westward tracked typhoon but also for the northward tracked one. The geopotential height increased in the east (area I) and decreased in the west (area II) (Fig.8a). That symbolizes barotropic waves. There is an obvious difference in area III between the two experiments, that is, there is a positive geopotential height difference in area III in the case of westward tracked typhoon, resulting in a westward stretching of the SAWP, but there is no obvious change of geopotential height in this area for the northward tracked typhoon. The positive geopotential height difference only appears in area I in the northeast of the typhoon (Fig.8b).

Now we analyze how the atmospheric circulation influences the propagation of this induced Rossby wave and why there is one positive geopotential height difference north of area II in Experiment 1 as shown in Fig.8. If the basic flow is $\bar{u} = \bar{u}(y)$, the barotropic linear Rossby wave equation with no horizontal divergence can be written as

$$(\frac{\partial}{\partial t} + \bar{u}\frac{\partial}{\partial x})\nabla_h^2\psi' + (\beta_0 - \frac{\partial^2\overline{u}}{\partial y^2})\frac{\partial\psi'}{\partial x} = 0. \quad (1)$$

If set

$$\psi' = \overline{\psi}(y)e^{ik(x-ct)} \quad (2)$$

and when $\overline{u} - c \neq 0$, then

$$\frac{\mathrm{d}^2\overline{\psi}}{\mathrm{d}y^2} + l^2\overline{\psi} = 0, \quad (3)$$

where $l^2 \equiv \frac{\beta_0 - \frac{\partial^2\overline{u}}{\partial y^2}}{\overline{u}-c} - k^2$ is the refraction index in the y direction. When $l^2 > 0$, the wave can propagate in the y direction (the equation has vibration solutions) to the area of the maximal refraction index. When

$l^2 < 0$, the Rossby wave is blocked off in the y direction.

There is a relationship of $l^2 = k_0^2 - k^2$ for stationary Rossby waves, where $k_0 = \sqrt{\frac{(\beta_0 - \frac{\partial^2 \overline{u}}{\partial y^2})}{\overline{u}}}$, thus the condition for the meridional propagation of stationary Rossby waves is $0 < \overline{u} < (\beta_0 - \frac{\partial^2 \overline{u}}{\partial y^2})/k^2$, that is to say, Rossby wave can transport in weak westerly wind but is blocked off in easterly wind. Figure 9 shows the vertical cross sections of the zonal wind in areas II and III along 122°E in Experiments 1 (Fig.9a) and 2 (Fig.9b) There is weak westerly wind in area II at mid-latitudes for the westward tracked typhoon (Fig.9a) and the induced Rossby waves by the typhoon can move across area II and propagate northward to area III, resulting in the increase of geopotential height and the westward stretching of the SAWP. But for the northward tracked typhoon, there is easterly wind in area II (Fig.9b) at mid-latitudes and the induced Rossby wave by the typhoon is blocked off and there is no westward stretching of the SAWP. We can conclude that the same initial disturbance of typhoon can induce different energy transport in different atmospheric circulations and therefore has different influences on mid-latitude circulations and the SAWP.

7. Conclusions and discussion

This paper verifies the traditional view that the SAWP has an important effect on typhoon tracks. Composite analyses show that when the tracks are westward, the SAWP has a zonal form with strong intensity in its western part and crosses a wide range of longitudes. The SAWP extends further west than it does with the other two kinds of typhoon tracks, and the westerly wind north of the SAWP is flat. When the tracks are recurving, the SAWP is in a zonal at

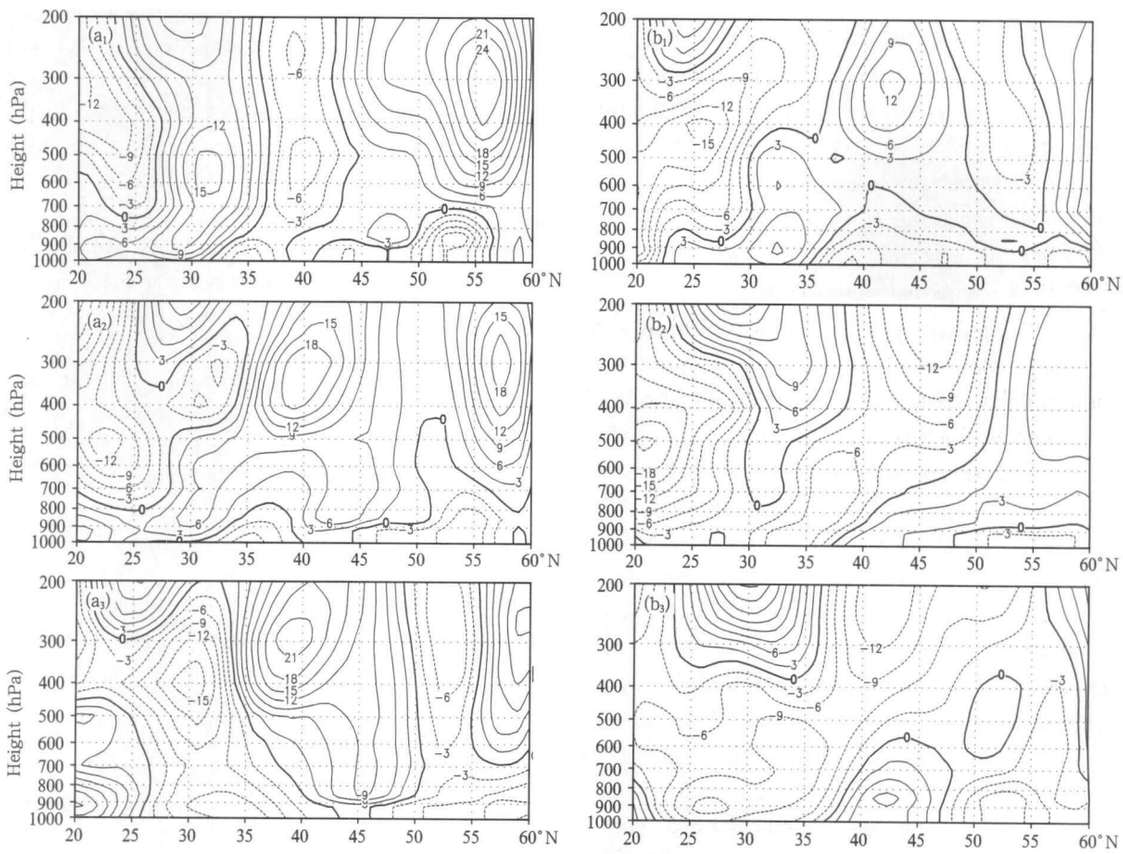

Fig.9. Vertical cross sections of the zonal wind (m s^{-1}) in areas II and III in Fig.8a along 122°E in Experiments 1 (a) and 2 (b) for day 2 (a_1,b_1), day 3(a_2,b_2), and day 4 (a_3,b_3). Dashed line: negative, solid line: positive, and thick line: zero contour.

first, and its eastern part weakens when the typhoon moves to the south of the SAWP, and strengthens during the recurving. There is also development of waves in the westerly wind north of the SAWP and two troughs, one is at 120°E and the other is in the middle of the Pacific Ocean. The SAWP weakens and then breaks in the central Pacific. When the tracks are northward, the intensity of the SAWP is the weakest and it is located far more east of its normal position, with its shape irregular. The typhoon moves northward across the middle part of the SAWP where the intensity is weak or the subtropical high is broken. The composite analyses also show that different types of typhoon tracks may have different effects on the variation of the SAWP.

In this paper, simulations are conducted to find out the interaction between typhoon and the SAWP by using the climate model R42L9. The results show that the typhoon moves westward under the circumstance of the flat easterlies south of a zonal SAWP corresponding to the westward tracked typhoon. When the easterly wind is weak and the SAWP is broken near Japan, the typhoon moves northward corresponding to the northward tracked typhoon. The conclusion by the simulations is consistent with the composite analyses. At the same time, the movement of the typhoon has an important effect on the variation of the SAWP. It affects not only the local area near the typhoon but also the far-away extratropical area by energy transport, thereby influencing the mid-high latitude circulations and the variation of the SAWP. There is one northeastward wave train for both the westward tracked typhoon and the northward tracked one, and their energy transport paths are almost the same. However, there is also a difference because of different backgrounds of atmospheric circulations. For the westward tracked typhoon, there are westerlies northwest of the typhoon, and the northward transport energy crossing this westerly wind area can strengthen the SAWP and makes it stretch to the west, thus preventing the northward movement of the typhoon. On the other hand, for the northward tracked typhoon, there is only one northeastward energy transport path, and there are easterlies northwest of the typhoon. The wave transport is blocked off meridionally, and the SAWP does not stretch to west, which facilitates the northward moving of the typhoon.

We can conclude that there are significant interactions between typhoon and the SAWP. Typhoon tracks are affected by the SAWP patterns and the typhoon induced strong disturbance can also influence the variation of the SAWP through energy dispersion. The climate model is suitable for studying the variation of the SAWP. And the numerical method by adding an ideal heating source to initiate a typhoon is feasible both in theory and in practice. But the question is that this low-resolution climate model can not simulate the intrinsic dynamic processes of the typhoon.

REFERENCES

Chan Johnny C. L., and William M. Gary, 1982: Tropical cyclone movement and surrounding flow relationships. *Mon. Wea. Rev.*, **110**(10), 1354–1374.

Chan Johnny C. L., 1985: Identification of the steering flow for tropical cyclone motion from objective analyzed wind fields. *Mon. Wea. Rev.*, **113**(1), 106–116.

Chen Lianshou and Luo Zhexian, 1995: Effect of the interaction of different-scale vortices on the structure and motion of typhoons. *Adv. Atmos. Sci.*, **12**(2), 207–214.

Chen Lianshou and Meng Zhiyong, 2001: An overview on tropical cyclone research progress in China during the past ten years. *Chinese J. Atmos. Sci.*, **25**(3), 420–432. (in Chinese)

Dong Keqin and Charles J. Neumann, 1983: On the relative motion of binary tropical cyclones. *Mon. Wea. Rev.*, **111**(5), 945–953.

Edward, B. Rodgers, Jong-Jin Baik, and Harold F. Pierce, 1994: The environmental influence on tropical cyclone precipitation. *Journal of Applied Meteorology*, **33**(5), 573–593.

Fan Yongxiang, 1996: *The summary of typhoon scientific operation test, the studies on typhoon scientific operation test and weather dynamic theory (one).* China Meteorological Press, Beijing, 113 pp. (in Chinese)

Geophysics Department of Peking University, meteorology teaching and research group, 1978: *Weather Analysis and Forecasting.* Science Press, Beijing, 570 pp. (in Chinese)

Harr, Patrick A., and Russell L. Elsberry, 1991: Tropical cyclone track characteristics as a function of large-scale circulation anomalies. *Mon. Wea. Rev.*,

119(6), 1448–1468.

Hoskins, B. J., and D. J. Karoly, 1981: The steady linear response of a spherical atmosphere to thermal and orographie forcing. *Journal of the atmospheric sciences*, **38**, 1179–1196.

Hoskins, B. J., M. E. Mclntyre, and A. W. Robertson, 1985: On the use and significance of isentropic potential vorticity maps. *Q. J. Roy. Meteor. Soc.*, **111**(470), 877–946.

Kalnay, E., and Coauthors, 1996: The NCEP/NCAR 40-year reanalysis project. *Bull. Amer. Meteor. Soc.*, **77**(3), 433–471.

Liu Bohan and Liang Chengli, 1987: A case study of typhoon Tess's (8515) Track. *Journal of Tropical Meteorology*, **3**(3), 251–257. (in Chinese)

Liu Hui and Wu Guoxiong, 1997: Impacts of land surface on climate of July and onset of summer monsoon: A study with an AGCM plus SSIB. *Adv. Atmos. Sci.*, **14**(3), 289–308.

Liu Shikuo and Liu Shida, 1991: *Atmospheric Dynamics.* Peking University Press, Beijing, 536 pp. (in chinese)

Liu Yimin, Wu Guoxiong, Liu Hui, et al., 1999: The effect of spatially nonuniform heating on the formation and variation of subtropical anticyclone. III: Condensation heating and South Asian anticyclone and western Pacific subtropical anticyclone. *Acta Meteor. Sinica*, **57**(5), 525–538. (in Chinese)

Liu Y. M., Wu G. X., Liu H., et al., 2001: Condensation heating of the Asian summer monsoon and the subtropical anticyclone in the Eastern Hemisphere. *Climate Dyn.*, **17**(4), 327–338.

Luo Zhexian, 2001: The effect of tropical cycolone on short term variation of subtropical anticyclone. *Acta Meteor. Sinica*, **59**(5), 549–559. (in Chinese)

Luo Zhexian and Ma Jingxian, 2001: Binary tropical cyclone interaction on the south of the subtropical anticyclone. *Acta Meteor. Sinica*, **59**(4), 450–458. (in Chinese)

Nikaidon, Y., 1989: The PJ-like north-south oscillations found in 4-month integrations of the global spectral model T42. *J. Meteor. Soc. Japan*, **67**, 687–604.

Qian Zhengcheng and Yu Shihua, 1991: The relationship between medium-range fluctuation of condensation heating in East Asia and quasi-2 weeks oscillation of the West Pacific subtropical anticyclone. *Journal of Tropical Meteorology*, **7**(3), 259–267. (in Chinese)

Rodwell, M. J., and B. J. Hoskins, 2001: Subtropical anticyclones and summer monsoons. *J. Climate*, **14**, 3192–3211.

Shi G. Y., 1981: An accurate calculation and the infrared transmission function of the atmospheric constituents. Ph.D. thesis, Dept. of Sci., Tohoku University of Japan.

Wang Zhilie, 1981: The influence of the westerly belt long-wave trough over Asia on the western Pacific typhoon tracks. *Chinese Journal of Atmospheric Sciences*, **5**(2), 198–205. (in Chinese)

Wang Zhilie, Hu Jian, and Ding Yihui, 1991: The effects of flow patterns over the northwest pacific on typhoon tracks. *Quarterly Journal of Applied Meteorology*, **2**(4), 362–368. (in Chinese)

Wu Guoxiong, Chou Jifan, Liu Yimin, et al., 2002: *Dynamic Issues on the Formation and Variation of Subtropical Anticyclone.* Science Press, Beijing, 314 pp. (in Chinese)

Wu Guoxiong, Liu Yimin, and Liu Ping, 1999: The effect of spatially nonuniform heating on the formation and variation of subtropical anticyclone. I: Scale analysis. *Acta Meteor. Sinica*, **57**(3), 257–263. (in Chinese)

Wu Guoxiong and Zhang Xuehong, 1997: Global ocean-atmosphere-land systerm model of LASG (GOALS/LASG) and its performance in simulation study. *J. Appl. Meteor.*, **8**(suppl.), 15–28. (in Chinese)

Wu Liguang and Wang Bin, 2000: A potential vorticity tendency diagnostic approach for tropical cyclone motion. *Mon. Wea. Rev.*, **128**(6), 1899–1911.

Wu T. W., Liu P., Wang Z. Zhi, et al. 2003: The performance of atmospheric component model (R42L9.0) of GOALS/LASG. *Advance Atmos. Sci.*, **20**(5), 726–742.

Xue Y. K., P. J. Sellers, J. L. Kinter, et al., 1991: A simplified biosphere model for global climate studies. *J. Climate*, **4**(3), 345–364.

Yang Meichuan and Zhu Yongti, 1998: Numerical experiment of tropical cyclone crossing the subtropical anticyclone. *Journal of Tropical Meteorology*, **14**(1), 85–90. (in Chinese)

Yu Shihua and Pan Chunsheng, 1989: An analysis of the circulation mechanism for the medium-rang advance and retreat of the West Pacific subtropical anticyclone. *Journal of Tropical Meteorology*, **5**(3), 220–225. (in Chinese)

Zhang Ren, Shi Hansheng, and Yu Shihua, 1995: Study on nonlinear stability of West Pacific subtropical anticyclone. *Chinese Journal of Atmospheric Sciences*, **19**(6), 687–700. (in Chinese)

Zhang X. H., Shi G. Y., Liu H., et al., 2000: *IAP Global Ocean-Atmosphere-Land System model.* Beijing, New York: Science Press, 252 pp.

Zhu Q. G., Lin J. R., Shou Sh. W., et al., 1992: *Meteorology Theory and Method.* China Meteorological Press, Beijing, 914 pp. (in Chinese)